Dynamic Queue-Aware RF Charging of Zero-Energy Devices via Reconfigurable Surfaces

Morteza Tavana, *Student Member, IEEE*, Zheng Chen, *Senior Member, IEEE*, and Emil Björnson, *Fellow, IEEE*

Abstract—Reconfigurable intelligent surfaces (RIS) can enhance wireless power transfer efficiency in communication networks by steering electromagnetic waves from a transmitter (TX) toward zero-energy devices (ZEDs) for charging their batteries. In this letter, we use the Lyapunov optimization framework to develop an algorithm that dynamically adjusts the TX power and RIS phase configuration based on the data queue lengths at the ZEDs. This approach aims to maintain queue stability while minimizing the average TX power. Our simulation results demonstrate that the proposed method provides stability and reduces the average TX power, whereas the queue-agnostic benchmark fails to achieve that even with much higher TX power.

Index Terms—Energy harvesting, Lyapunov optimization, reconfigurable intelligent surfaces, zero-energy devices.

I. Introduction

THE EXPANSION of wireless networks to accommodate massive Internet of Things (IoT) devices underscores the importance of developing energy-efficient and cost-effective solutions for the deployment and maintenance of these devices [1]. Zero-energy devices (ZEDs), which can harvest energy from their surrounding environment, eliminate the need for battery replacement or manual charging. The integration of radio frequency (RF) remote charging into this ecosystem offers a sustainable, cost-effective, and innovative solution, aligning with the demands of future wireless networks.

There are two main categories of RF wireless power transfer (WPT): simultaneous wireless information and power transfer (SWIPT) [2], predominantly designed for downlink transmission, and wirelessly powered communication networks [3], which can be used for both uplink and downlink operations. A key obstacle in RF WPT for ZEDs is the high path loss, which severely limits the power transfer efficiency. Path losses in wireless channels often exceed 60 dB, whereas the beamforming gain from a 10^M-element antenna array is $10M$ dB [4]. As a result, relying solely on energy beamforming techniques falls short of ensuring efficient WPT, unless massive numbers of antenna elements are deployed. However, the deployment of a large antenna array for energy beamforming is challenging, as each antenna element requires an RF chain, which increases the hardware complexity and power consumption.

With the emergence of reconfigurable intelligent surface (RIS), it becomes possible to control the propagation environment to enhance the communication quality. RISs are generally composed of passive elements capable of manipulating electromagnetic (EM) waves by adding adjustable phase shifts, without the need for active RF components [5]. The hardware of a RIS is much simpler than that of active antenna arrays, making RIS a more practical and cost-effective solution.

In the context of WPT, a RIS can collect the RF power, either from dedicated power sources or ambient sources, and passively beamform it toward ZEDs. The delivered power grows quadratically with the surface area of the RIS [5]. A RIS-assisted SWIPT system was introduced in [6], where a multi-antenna access point serves multiple devices for information decoding or energy harvesting (EH) through a RIS. In [7], an amplitude-based sequential optimization algorithm for EH with RIS is proposed to enable zero-energy RIS without the need for coordination with the ambient RF power source. In [8], a dynamic data power control and scheduling algorithm is proposed for uplink multi-antenna systems with random data arrivals, using the Lyapunov optimization method. A static remote powering scheme where a RIS and ZEDs harvest energy from a transmitter is considered in [9]. The goal is to minimize the transmit power under channel uncertainties.

A ZED can only transmit data packets when its battery is charged. Otherwise newly generated data packets will be accumulated in the data queue, causing increasing queueing delay. To achieve quality of service and prevent overflow, the aim of RF charging should be to provide the ZEDs with sufficient power to maintain stable data queues, which implies finite queueing delay. To the best of our knowledge, this is the first paper to consider queue-aware RF charging of ZEDs with the assistance of RIS. We address the problem by considering the dynamic adjustment of the transmitter (TX) power and RIS phases based on the current queue information. The main contributions are:

- We propose a framework for dynamic, queue-aware RF charging of ZEDs with the assistance of a RIS. We formulate an optimization problem to maintain data queue stability while minimizing the average TX power.
- We present a Lyapunov-based queue-aware algorithm for dynamic TX power control and RIS phase configuration. We propose a simplified scheduling algorithm offering slightly lower power efficiency but reduced complexity.
- Simulation results highlight the importance of utilizing queue information in dynamic RF charging schemes.
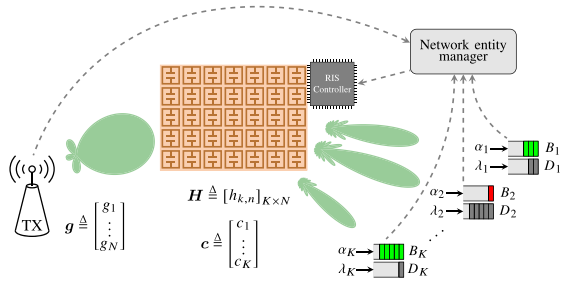
Fig. 1.   RIS-assisted energy harvesting for ZEDs.

Notations: We denote the sets of non-negative integers and real numbers with $\mathbb{N}_0$ and $\mathbb{R}$, respectively. Vectors are indicated by lower-case bold-face letters, e.g., $\boldsymbol{x}$, and x_i denotes the *i*th element of $\boldsymbol{x}$. We represent matrices by upper-case bold-face letters, e.g., $\boldsymbol{A}$, and $[\boldsymbol{A}]_{m,n}$ indicates the element of $\boldsymbol{A}$ with row number *m* and column number *n*. We represent the conjugate of *z* with z^*. We denote the optimal solution with the superscript $\star$, e.g., $x^\star$. The operation $\text{Arg}(z)$ returns the principal value of the argument of *z* that lies within the interval $(-\pi, \pi]$. The indicator function is denoted by $\mathbb{1}(\cdot)$.

II. System Model and Problem Formulation

We consider the problem of charging multiple ZEDs with RF energy harvesting assisted by a RIS. The setup is illustrated in Fig. 1. Our system consists of a TX, a RIS with *N* elements, and *K* ZEDs. Each ZED is equipped with a small battery (or capacitor) to store energy for future usage. Additionally, a network entity manager (NEM) communicates with different entities (e.g., RIS, TX, and ZEDs) and provides the necessary inputs to the RIS controller, such as the data queue statuses of the ZEDs and the channel state information (CSI).[1]

The complex channel gain vector between the TX and the ZED is denoted as $\boldsymbol{c} \triangleq [c_1, c_2, \ldots, c_K]^{\mathsf{T}}$. The complex channel gain vector between the TX and the RIS elements is represented as $\boldsymbol{g} \triangleq [g_1, g_2, \ldots, g_N]^{\mathsf{T}}$. We further assume that the complex channel gain matrix between the RIS elements and ZEDs is denoted as $\boldsymbol{H}$, where $[\boldsymbol{H}]_{k,n}$ is the complex channel gain between the ZED *k* and the RIS element *n*.

We consider a slotted time framework where each time slot corresponds to a duration of T_s seconds. We assume that the time slot *t*, where *t* is a non-negative integer, refers to the time interval $[t \cdot T_s, (t+1) \cdot T_s)$. The channel gains within each time slot are assumed to be static but can vary over different slots. For all $1 \leq k \leq K$, the overall path gain between the TX and the ZED *k* is given by

$$f_k(\boldsymbol{\vartheta}) \triangleq \left| c_k + \sum_{n=1}^{N} g_n [\boldsymbol{H}]_{k,n} e^{j\vartheta_n} \right|^2. \tag{1}$$

We assume that the data arrivals at ZED *k*, for all $1 \leq k \leq K$, follow Bernoulli distributions; e.g., one packet arrives in each slot with probability λ_k, and there is no arrival with

probability $1 - \lambda_k$. Furthermore, each time the ZED *k* transmits a data packet, it consumes δ_k Joules.

1) Battery Level Evolution: The battery level of each ZED is divided into discrete energy chunks where each chunk corresponds to the amount of energy consumed by one data packet transmission, δ_k. Let $B_k(t)$ denote the battery level at the beginning of the time slot *t*. During the time slot *t*, the amount of transferred energy to ZED *k* is

$$\gamma_k(t) \triangleq p(t) \cdot f_k(\boldsymbol{\vartheta}(t)) \cdot T_s, \tag{2}$$

where $\boldsymbol{\vartheta}(t) = [\vartheta_1(t), \vartheta_2(t), \ldots, \vartheta_N(t)]^{\mathsf{T}}$ and $p(t)$ are the RIS phase vector and TX power in slot *t*, respectively [5]. Moreover, the energy units harvested by the ZED *k* is

$$\alpha_k(t) \triangleq \frac{\gamma_k(t)}{\delta_k}. \tag{3}$$

Therefore, for the ZED *k*, the battery evolves as

$$B_k(t+1) = \max\{B_k(t) - \mathbb{1}(D_k(t) > 0), 0\} + \alpha_k(t), \tag{4}$$

where $D_k(t)$ is the data queue length of the ZED *k*.

2) Data Queue Evolution: The data queue of the ZED *k* for all $1 \leq k \leq K$ evolves as

$$D_k(t+1) = \max\{D_k(t) - \mathbb{1}(B_k(t) \geq 1), 0\} + A_k(t), \tag{5}$$

where

$$A_k(t) = \begin{cases} 1, & \text{One packet arrival with probability } \lambda_k, \\ 0, & \text{No arrival with probability } 1 - \lambda_k. \end{cases} \tag{6}$$

The main objective is to dynamically control the phases of the RIS and the TX power to minimize the average power consumption of the TX while keeping the data queues of the ZEDs stable. To achieve this, we formulate the stochastic optimization problem

$$\begin{aligned} \underset{\{p(t), \boldsymbol{\vartheta}(t)\}_{t=0,\ldots}}{\text{minimize}} \quad & \limsup_{T \to \infty} \frac{1}{T} \sum_{t=0}^{T-1} \mathbb{E}(p(t)) \\ \text{subject to} \quad & \limsup_{T \to \infty} \frac{1}{T} \sum_{t=0}^{T-1} \mathbb{E}(D_k(t)) < \infty \; \forall k, \\ & B_k(\cdot) \text{ evolves as (4) } \forall k, \\ & D_k(\cdot) \text{ evolves as (5) } \forall k, \\ & p : \mathbb{N}_0 \to [0, p_{\max}], \\ & \boldsymbol{\vartheta} : \mathbb{N}_0 \to (0, 2\pi)^N, \end{aligned} \tag{7}$$

where $p(\cdot)$ and $\boldsymbol{\vartheta}(\cdot)$ are the control variables, and $\{B_k(\cdot)\}_{k=1}^{K}$ and $\{D_k(\cdot)\}_{k=1}^{K}$ are the state variables. The solution to this problem is an algorithm that determines the control variables $p(t)$ and $\boldsymbol{\vartheta}(t)$ in each time slot such that the long-term constraints are satisfied and that the long-term energy consumption is minimized.

III. Dynamic Queue-Aware Scheduling

In this section, we present our dynamic queue-aware RF charging algorithm obtained by solving the problem defined in (7) using the Lyapunov optimization framework.

A. Lyapunov Drift

Let $\boldsymbol{D}(t) \triangleq [D_1(t), D_2(t), \ldots, D_K(t)]^{\mathsf{T}}$ be the queue state vector in slot *t*. We define the Lyapunov function as

$$L(\boldsymbol{D}(t)) \triangleq \frac{1}{2} \sum_{k=1}^{K} D_k^2(t), \tag{8}$$

---

[1]In a stationary environment with no moving objects, the channels remain static during the operation. Consequently, CSI can be obtained using the known positions of the entities or through channel estimation techniques. We assume perfect CSI to focus on queue-aware scheduling design. However, if there are CSI errors in practice, the resulting imperfect phase configuration will lead to somewhat lower path gains, which can be compensated for by increasing the transmit power or adding more RIS elements.

where a small $L(\boldsymbol{D}(t))$ implies a small data backlog, while a large $L(\boldsymbol{D}(t))$ implies that at least one data queue is large [10]. We define the one-step conditional Lyapunov drift as

$$\Delta(\boldsymbol{D}(t)) \triangleq \mathbb{E}(L(\boldsymbol{D}(t+1)) - L(\boldsymbol{D}(t)) \mid \boldsymbol{D}(t))$$

$$= \frac{1}{2} \sum_{k=1}^{K} \mathbb{E}\Big((\max\{D_k(t) - b_k(t), 0\} + A_k(t))^2 - D_k^2(t) | D_k(t) \Big)$$

$$\leq \sum_{k=1}^{K} \mathbb{E}\left(\frac{A_k^2(t) + b_k^2(t)}{2} + D_k(t)(A_k(t) - b_k(t)) | D_k(t) \right)$$

$$\overset{(a)}{\leq} C - \sum_{k=1}^{K} D_k(t) q_k(t), \tag{9}$$

where $C \triangleq 0.5K + \sum_{k=1}^{K} \lambda_k(0.5 + D_k(t))$, $b_k(t) \triangleq \mathbb{1}(B_k(t) \geq 1)$ and $q_k(t) = \mathbb{E}[b_k(t)|D_k(t)] = \Pr[B_k(t) \geq 1]$. Moreover, in (a), we utilize the fact that $b_k^2(t) \leq 1$ and $\mathbb{E}(A_k^2) = \mathbb{E}(A_k) = \lambda_k$.

B. Min-Drift-Plus-Penalty

Based on the Lyapunov drift, we obtain the following bound on the Drift-Plus-Penalty (DPP):

$$\text{DPP} \triangleq \Delta(\boldsymbol{D}(t)) + V \cdot \mathbb{E}(p(t) \mid \boldsymbol{D}(t))$$

$$\leq C + \mathbb{E}\left(V \cdot p(t) - \sum_{k=1}^{K} D_k(t) \cdot q_k(t) | \boldsymbol{D}(t) \right), \tag{10}$$

where $V > 0$ is a design parameter that can be selected to balance latency variations versus power minimization. Finally, by greedily minimizing the term inside the conditional expectation, we obtain the following per-slot optimization problem:

$$\underset{p(t), \boldsymbol{\vartheta}(t)}{\text{minimize}} \quad V \cdot p(t) - \sum_{k=1}^{K} D_k(t) \cdot q_k(t)$$

$$\text{subject to } 0 \leq p(t) \leq p_{\max},$$

$$\boldsymbol{\vartheta}(t) \in [0, 2\pi)^N. \tag{11}$$

Note that the probability $q_k(t) = \Pr[B_k(t) \geq 1]$ of being charged depends on the RF charging process and the configured parameters $p(t)$ and $\boldsymbol{\vartheta}(t)$.

C. Proposed Two-Step Optimization Algorithm

Solving (11) is challenging since there is no direct mapping between the value of $q_k(t)$ and the control variables. However, from (3) and (4), it can be observed that $B_k(t)$ monotonically increases with the charging power $\gamma_k(t)$, which also makes $q_k(t)$ an increasing function of $\gamma_k(t)$. Thus, by replacing $q_k(t)$ with $p(t) \cdot f_k(\boldsymbol{\vartheta}(t))$ in (11), we can obtain a simplified problem as

$$\underset{p(t), \boldsymbol{\vartheta}(t)}{\text{minimize}} \quad p(t) \cdot \left(V - \sum_{k=1}^{K} D_k(t) \cdot f_k(\boldsymbol{\vartheta}(t)) \right)$$

$$\text{subject to } 0 \leq p(t) \leq p_{\max},$$

$$\boldsymbol{\vartheta}(t) \in [0, 2\pi)^N. \tag{12}$$

We propose to minimize (12) with respect to the $p(t)$ and $\boldsymbol{\vartheta}(t)$ in the following two steps.

1) Phase Configuration: First, we find the optimal $\boldsymbol{\vartheta}(t)$ that solves the following optimization problem:

$$\underset{\boldsymbol{\vartheta}(t)}{\text{maximize}} \quad \sum_{k=1}^{K} D_k(t) \cdot \left| c_k + \sum_{n=1}^{N} g_n[\boldsymbol{H}]_{k,n} e^{j\vartheta_n(t)} \right|^2$$

$$\text{subject to } \boldsymbol{\vartheta}(t) \in [0, 2\pi)^N. \tag{13}$$

In each time slot t, we define $\boldsymbol{x} \triangleq [e^{-j\vartheta_1(t)}, e^{-j\vartheta_2(t)}, \ldots, e^{-j\vartheta_N(t)}]^\mathsf{T}$, $w_k \triangleq D_k(t) \ \forall 1 \leq k \leq K$, and $\boldsymbol{z}_k \triangleq [g_1[\boldsymbol{H}]_{k,1}, g_2[\boldsymbol{H}]_{k,2}, \ldots, g_N[\boldsymbol{H}]_{k,N}]^\mathsf{T}$. Therefore, (13) is equivalent to

$$\underset{\boldsymbol{x}}{\text{maximize}} \quad \sum_{k=1}^{K} w_k \left| c_k + \boldsymbol{x}^\mathsf{H} \boldsymbol{z}_k \right|^2 \tag{14a}$$

$$\text{subject to } |x_n| = 1, \quad \forall 1 \leq n \leq N. \tag{14b}$$

The equality constraints (14b) are non-convex. But the objective function is convex with respect to $\boldsymbol{x}$. We apply the successive convex approximation (SCA) technique to obtain a stationary point for (14). We have

$$\sum_{k=1}^{K} w_k \left| c_k + \boldsymbol{x}^\mathsf{H} \boldsymbol{z}_k \right|^2$$

$$= \boldsymbol{x}^\mathsf{H} \boldsymbol{Z} \boldsymbol{x} + 2 \sum_{k=1}^{K} w_k \operatorname{Re}\left(\boldsymbol{x}^\mathsf{H} \boldsymbol{z}_k c_k^* \right) + \sum_{k=1}^{K} w_k |c_k|^2$$

$$\overset{(a)}{\geq} 2 \operatorname{Re}\left(\boldsymbol{x}^\mathsf{H} \left(\boldsymbol{Z} \boldsymbol{x}_0 + \sum_{k=1}^{K} w_k \boldsymbol{z}_k c_k^* \right) \right)$$

$$- \boldsymbol{x}_0^\mathsf{H} \boldsymbol{Z} \boldsymbol{x}_0 + \sum_{k=1}^{K} w_k |c_k|^2, \tag{15}$$

where $\boldsymbol{Z} \triangleq \sum_{k=1}^{K} w_k \boldsymbol{z}_k \boldsymbol{z}_k^\mathsf{H}$. The inequality (a) holds as $\boldsymbol{Z}$ is a positive definite matrix. Moreover, equality in (a) is achieved at the point $\boldsymbol{x} = \boldsymbol{x}_0$. The optimization problem becomes

$$\underset{\boldsymbol{x}}{\text{maximize}} \operatorname{Re}\left(\boldsymbol{x}^\mathsf{H} \boldsymbol{v} \right)$$

$$\text{subject to } |x_n| = 1, \quad \forall 1 \leq n \leq N, \tag{16}$$

where $\boldsymbol{v} \triangleq \boldsymbol{Z} \boldsymbol{x}_0 + \sum_{k=1}^{K} w_k \boldsymbol{z}_k c_k^*$. It is easy to show that the optimal solution to the problem (16) is

$$x_n \triangleq \begin{cases} 1, & v_n = 0, \\ \frac{v_n}{|v_n|}, & v_n \neq 0. \end{cases} \tag{17}$$

We repeat this procedure by setting $\boldsymbol{x}_0 = \boldsymbol{x}$ until it converges to a stationary point. The resulting solution is $\boldsymbol{\vartheta}^\star \triangleq \operatorname{Arg}(\boldsymbol{x}^*)$.

2) Power Configuration: We substitute $\boldsymbol{\vartheta}^\star(t)$ in (12) and minimize the following problem with respect to $p(t)$:

$$\underset{p(t)}{\text{minimize}} \quad p(t) \cdot \left(V - \sum_{k=1}^{K} D_k(t) \cdot f_k(\boldsymbol{\vartheta}^\star(t)) \right)$$

$$\text{subject to } 0 \leq p(t) \leq p_{\max}. \tag{18}$$

The optimum variable for (18) is

$$p^\star(t) = \begin{cases} 0, & V > \sum_{k=1}^{K} D_k(t) \cdot f_k(\boldsymbol{\vartheta}^\star(t)), \\ p_{\max}, & \text{otherwise}. \end{cases} \tag{19}$$

In a dynamic scenario, the NEM periodically receives the updates on the data queues and the identity indices of the ZEDs.[2] Then, it dynamically updates the RIS phase vector and the TX power according to Algorithm 1. In this algorithm, for the weighted-sum power maximization, the process is repeated to reach a convergence accuracy of $\varepsilon > 0$. This means that the ratio between the weighted-sum power in the last iteration and the one in the previous iteration is less than $1 + \varepsilon$.

---

[2] If a queue length hasn't changed in a specific time period, no update needs to be sent.

Algorithm 1: Lyapunov Queue-Aware Scheduling

1   **Input:** The number of RIS elements N, convergence accuracy $\varepsilon > 0$, c, g, H, and the parameter V.
2   **Output:** RIS phase vector $\boldsymbol{\vartheta}^\star(\cdot)$ and TX power $p^\star(\cdot)$ over time.
3   **Initialize:** $t \leftarrow 0$,
4   **for** $k \leftarrow 1$ **to** K **do**
5     $\boldsymbol{z}_k \leftarrow \left[g_1[\boldsymbol{H}]_{k,1}, g_2[\boldsymbol{H}]_{k,2}, \ldots, g_N[\boldsymbol{H}]_{k,N} \right]^{\mathsf{T}}$;
6   **end**
7   **while** $t \geq 0$ **do**
8   **if** *any update on the data queues* **then**
9       $\boldsymbol{Z} \leftarrow \sum_{k=1}^{K} D_k(t) \boldsymbol{z}_k \boldsymbol{z}_k^{\mathsf{H}}$;
10      $\boldsymbol{\varphi} \leftarrow$ a random initial vector;
11      $\boldsymbol{x} \leftarrow \left[e^{-j\varphi_1}, e^{-j\varphi_2}, \ldots, e^{-j\varphi_N} \right]^{\mathsf{T}}$;
12      $s_{\mathrm{o}} \leftarrow 0^+$;
13      $s \leftarrow \sum_{k=1}^{K} D_k(t) \left| c_k + \boldsymbol{x}^{\mathsf{H}} \boldsymbol{z}_k \right|^2$;
14   **while** $s/s_{\mathrm{o}} - 1 > \varepsilon$ **do**
15        $s_{\mathrm{o}} \leftarrow s$;
16        $\boldsymbol{v} \leftarrow \boldsymbol{Z}\boldsymbol{x} + \sum_{k=1}^{K} D_k(t) \boldsymbol{z}_k c_k^*$;
17   **for** $n \leftarrow 1$ **to** N **do**
18   Update x_n according to (17);
19   **end**
20        $s \leftarrow \sum_{k=1}^{K} D_k(t) \left| c_k + \boldsymbol{x}^{\mathsf{H}} \boldsymbol{z}_k \right|^2$;
21   **end**
22      $\boldsymbol{\vartheta}^\star(t) \leftarrow \mathrm{Arg}\left(\boldsymbol{x}^* \right)$;
23   Update $p^\star(t)$ according to (19);
24   **else**
25      $\boldsymbol{\vartheta}^\star(t) \leftarrow \boldsymbol{\vartheta}^\star(t-1)$;
26      $p^\star(t) \leftarrow p^\star(t-1)$;
27   **end**
28   Battery levels evolve as (4);
29   Data queues evolve as (5);
30     $t \leftarrow t + 1$;
31 **end**

Algorithm 2: Heuristic Queue-Aware Scheduling

1   **Input:** The number of RIS elements N, c, g, H, and the parameter V.
2   **Output:** RIS phase vector $\boldsymbol{\vartheta}^\star(\cdot)$ and TX power $p^\star(\cdot)$ over time.
3   **Initialize:** $t \leftarrow 0$,
4   **for** $k \leftarrow 1$ **to** K **do**
5     $\boldsymbol{z}_k \leftarrow \left[g_1[\boldsymbol{H}]_{k,1}, g_2[\boldsymbol{H}]_{k,2}, \ldots, g_N[\boldsymbol{H}]_{k,N} \right]^{\mathsf{T}}$;
6   **end**
7   **while** $t \geq 0$ **do**
8   **if** *any update on the data queues* **then**
9      $k \leftarrow \underset{i}{\mathrm{argmax}}\ D_i$;
10      $\boldsymbol{\vartheta}^\star(t) \leftarrow \mathrm{Arg}\left(c_k \boldsymbol{z}_k^* \right)$;
11   Update $p^\star(t)$ according to (19);
12   **else**
13      $\boldsymbol{\vartheta}^\star(t) \leftarrow \boldsymbol{\vartheta}^\star(t-1)$;
14      $p^\star(t) \leftarrow p^\star(t-1)$;
15   **end**
16   Battery levels evolve as (4);
17   Data queues evolve as (5);
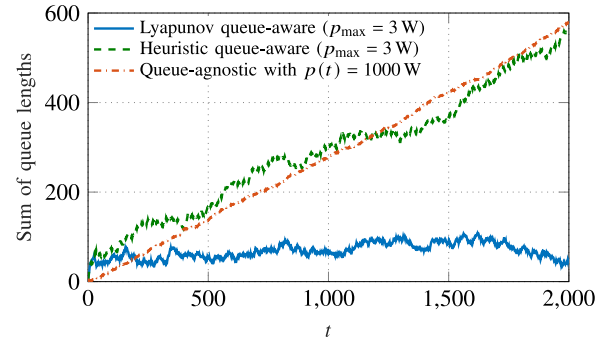18 $t \leftarrow t + 1$;
19 **end**

Fig. 2. The variation of the sum of queue lengths over time for different methods.

TABLE I
PERFORMANCE COMPARISON

Method	Average TX power	Sum of queue lengths	
		$t = 1000$	$t = 100000$
Lyapunov queue-aware	2.98 W ($p_{\max}=3$ W)	42	53
Heuristic queue-aware	3 W ($p_{\max}=3$ W)	306	22376
Lyapunov queue-aware	3.04 W ($p_{\max}=4$ W)	31	30
Heuristic queue-aware	3.21 W ($p_{\max}=4$ W)	48	45
Queue-agnostic	1000 W	283	29794

IV. PERFORMANCE EVALUATION

In this section, we demonstrate the performance of our proposed dynamic RF charging algorithm. We consider a RIS with $N = 100$ elements[3] and $K = 10$ ZEDs. This setup could represent a home or office room that contains many zero-energy sensors. We assume $\delta_k = 9\,\mu$J for all $1 \leq k \leq K$.

We consider a scenario where a RIS is situated in the xy plane, with its center positioned at the origin. The elements form a grid with half-wavelength spacing, where we consider a wavelength of 0.125 m. The RIS occupies an area of $0.39\,\mathrm{m}^2$. Furthermore, we consider an isotropic RF source at $[0, -2, 3]^{\mathsf{T}}$ m and the positions of the EH devices are realizations of the random vector $[X, -0.625, Z]^{\mathsf{T}}$ m, where $X \sim \mathcal{U}(-1.5, 1.5)$ and $Z \sim \mathcal{U}(1, 4)$. We compute the channel gains between the RIS elements and the transmit and receive antennas by taking into account the radiative near-field and polarization effects [11]. For the ZED k, the channel gain with optimal RIS configuration is $||c_k| + \sum_{n=1}^{N} |g_n[\boldsymbol{H}]_{k,n}||$. We assign indices to the ZEDs such that each kth ZED corresponds to the kth smallest optimal channel gain. We assume data arrivals with $\lambda_k = 0.09 \cdot k$ for each $1 \leq k \leq K$.

For performance comparison, we also consider a simplified heuristic queue-aware method. The approach is to dynamically adjust the RIS phases to maximize the received power at the ZED with the currently largest data queue length. This technique is more straightforward than the weighted-sum power maximization method in Algorithm 1, as it allows for a closed-form solution. To optimize the received power at the ZED k, for $1 \leq k \leq K$, the RIS phases are to be set as follows:

$$\boldsymbol{\vartheta} = \mathrm{Arg}\left(c_k \left[g_1[\boldsymbol{H}]_{k,1}, \ldots, g_N[\boldsymbol{H}]_{k,N} \right]^{\mathsf{H}} \right). \quad (20)$$

This approach is detailed in Algorithm 2. The TX power control is identical to the one in Algorithm 1.

Furthermore, we consider a queue-agnostic benchmark without considering queue information. In this approach, which is a simplified version of the method proposed in [6], the TX power remains constant, and the RIS phases are adjusted to maximize the sum power received by the ZEDs.

---

[3]We consider a fixed N as in practice. The harvested power grows with N for all ZEDs, while the proposed algorithm determines which ZEDs get extra transmit beamforming gain depending on their current queue lengths.
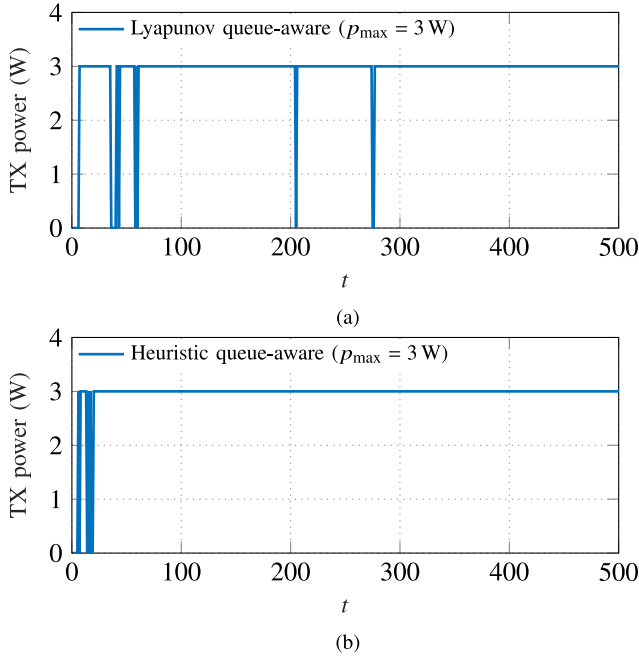
Fig. 3. The variation of the TX power over time for (a) Lyapunov queue-aware (b) heuristic queue-aware methods.

Fig. 2 and Fig. 3 illustrate the variation of the sum of queue lengths and the TX power over time for different methods in a single-run simulation. In this simulation, to maintain small queue lengths, we set $V = 0.1$. Moreover, for the proposed queue-aware methods, we considered a maximum TX power of $p_{\max} = 3$ W. In this setup, among the evaluated methods, only the Lyapunov-based queue-aware scheduling achieves stable queues. In contrast, the heuristic queue-aware method fails to maintain stable queues at $p_{\max} = 3$ W, as seen from the linearly growing queue lengths. For the queue-agnostic approach, a significantly higher TX power of $p(t) = 1000$ W was used, yet we still observed the trend of unstable queues where the queue length grows unboundedly with time. Fig. 3 shows that in the queue-aware methods, the TX power increases to $p_{\max}$ whenever the queues grow. Comparing the Lyapunov and heuristic queue-aware methods for $p_{\max} = 3$ W in Fig. 3(a) and Fig. 3(b), we observe that the latter method keeps the TX power at its maximum after a certain initial time, which suggests its difficulties in stabilizing the queues. On the other hand, the former method frequently reduces the TX power to zero, indicating its superior ability to maintain queue stability over extended periods. Additionally, the former method demonstrates a slight power efficiency advantage.

To evaluate the long-term stability of the considered methods, we present the sum of queue lengths at $t = 100000$ in Table I. It is observed that at $p_{\max} = 3$ W, only the Lyapunov-based scheduling method maintains queue stability.

However, at $p_{\max} = 4$ W, both the Lyapunov and heuristic queue-aware scheduling methods succeed in stabilizing the queues. Notably, the average TX power for the former is slightly lower than that of the latter. Additionally, the fact that the queue-agnostic method at a significantly higher TX power of $p(t) = 1000$ W fails to provide stable queues, while the queue-aware methods achieve stability at much lower power, demonstrates the importance of incorporating queue information in the dynamic RF charging algorithm.

V. CONCLUSION

We considered a scenario of RIS-assisted RF charging where multiple ZEDs rely on harvested energy to transmit data packets that are randomly generated over time.

We proposed two algorithms that adapt the TX power and RIS phase configuration based on the current queue states of the ZED. These queue-aware methods outperform the queue-agnostic approach in maintaining stable queues. The Lyapunov-based method demonstrates greater efficiency in most scenarios and generally consumes a lower average TX power than the heuristic method.

REFERENCES

[1] S. Sinha. "State of the IoT 2023." 2023. [Online]. Available: https://iot-analytics.com/number-connected-iot-devices/

[2] R. Zhang and C. K. Ho, "MIMO broadcasting for simultaneous wireless information and power transfer," *IEEE Trans. Wireless Commun.*, vol. 12, no. 5, pp. 1989–2001, May 2013.

[3] H. Ju and R. Zhang, "Throughput Maximization in wireless powered communication networks," *IEEE Trans. Wireless Commun.*, vol. 13, no. 1, pp. 418–428, Jan. 2014.

[4] T. L. Marzetta, E. G. Larsson, and H. Yang, *Fundamentals of Massive MIMO*. Cambridge, U.K.: Cambridge Univ. Press, 2016.

[5] E. Björnson, H. Wymeersch, B. Matthiesen, P. Popovski, L. Sanguinetti, and E. De Carvalho, "Reconfigurable intelligent surfaces: A signal processing perspective with wireless applications," *IEEE Signal Process. Mag.*, vol. 39, no. 2, pp. 135–158, Mar. 2022.

[6] Q. Wu and R. Zhang, "Weighted sum power maximization for intelligent reflecting surface aided SWIPT," *IEEE Wireless Commun. Lett.*, vol. 9, no. 5, pp. 586–590, May 2020.

[7] M. Tavana, M. Masoudi, and E. Björnson, "Energy harvesting maximization for reconfigurable intelligent surfaces using amplitude measurements," *IEEE Trans. Commun.*, vol. 72, no. 4, pp. 2201–2215, Apr. 2024.

[8] Z. Chen, E. Björnson, and E. G. Larsson, "Dynamic resource allocation in co-located and cell-free massive MIMO," *IEEE Trans. Green Commun. Netw.*, vol. 4, no. 1, pp. 209–220, Mar. 2020.

[9] Y. Zheng, S. A. Tegos, Y. Xiao, P. D. Diamantoulakis, Z. Ma, and G. K. Karagiannidis, "Zero-energy device networks with wireless-powered RISs," *IEEE Trans. Veh. Technol.*, vol. 72, no. 10, pp. 13655–13660, Oct. 2023.

[10] M. Neely, *Stochastic Network Optimization With Application to Communication and Queueing Systems*. Cham, Switzerland: Springer Nat., 2022.

[11] E. Björnson and L. Sanguinetti, "Power scaling laws and near-field behaviors of massive MIMO and intelligent reflecting surfaces," *IEEE Open J. Commun. Soc.*, vol. 1, pp. 1306–1324, 2020.